

## Free vibration of functionally graded thin beams made of saturated porous materials

M.R. Galeban<sup>1a</sup>, A. Mojahedin<sup>\*2</sup>, Y. Taghavi<sup>3</sup> and M. Jabbari<sup>2</sup>

<sup>1</sup> Young Researchers and Elite Club Behbahan Branch, Islamic Azad University, Behbahan, Iran

<sup>2</sup> Department of Mechanical Engineering, South Tehran Branch, Islamic Azad University, Tehran, Iran

<sup>3</sup> Department of Biomedical Engineering, Tehran Medical Sciences Branch, Islamic Azad University, Tehran, Iran

(Received August 11, 2015, Revised January 25, 2016, Accepted July 04, 2016)

**Abstract.** This study presents free vibration of beam made of porous material. The mechanical properties of the beam is variable in the thickness direction and the beam is investigated in three situations: poro/nonlinear nonsymmetric distribution, poro/nonlinear symmetric distribution, and poro/monotonous distribution. First, the governing equations of porous beam are derived using principle of virtual work based on Euler-Bernoulli theory. Then, the effect of pores compressibility on natural frequencies of the beam is studied by considering clamped-clamped, clamped-free and hinged-hinged boundary conditions. Moreover, the results are compared with homogeneous beam with the same boundary conditions. Finally, the effects of poroelastic parameters such as pores compressibility, coefficients of porosity and mass on natural frequencies has been considered separately and simultaneously.

**Keywords:** free vibration; Euler-Bernoulli theory; functionally graded beam; porous material

### 1. Introduction

Recently, by development of technology in construction and application of pieces such as shell, plate and beam in this area the especial properties of these structures have gained particular attentions in engineering construction. More than ever the demand for manufacturing lightweight components with capabilities and special properties such as flexibility, higher resistance against reducing the mass of the material, higher resistance to crack propagation, especial usage of mechanical and thermal properties of materials and etc. in the vibration system such as space industry application, the transport industry and etc. is felt. Hence, the study of behavior of these pieces with functional material is necessary. Functional materials are generally characterized as the materials which their mechanical, electrical, thermal and etc. properties vary across one or more directions. The properties of these materials may be changed by properties of the layers texture or as a result of the existence of pores in material structure which properties and distribution of pores affect on functional material properties. In recent years many researchers have investigated vibration behavior of beam with the functional properties. For example, Murin *et al.* (2010)

---

\*Corresponding author, M.Sc., E-mail: [mojahedin.arvin@gmail.com](mailto:mojahedin.arvin@gmail.com)

<sup>a</sup> M.Sc., E-mail: [mohammadreza.galeban@gmail.com](mailto:mohammadreza.galeban@gmail.com)

derived a fourth-order differential equation of the functionally graded beam deflection with variable material properties across the thickness. The linear beam theory has been used for establishing the equilibrium and kinematic equations of the functionally graded beam. The shear force deformation effect and the effect of consistent mass distribution and mass inertia moment have been taken into account, too. Finally, numerical experiments were performed to calculate the eigen frequencies and corresponding eigen modes of one-layer beams and multilayered functionally graded material (FGM) sandwich beams. Aminbaghai *et al.* (2011) investigated modelling and simulation of free vibration of the 2D FGM beams with continuous spatial variation of material properties. The fourth-order differential equation of the second order beam theory has been presented which was used in modal analysis with effect of large axial force. The effect of shear force deformation, consistent mass distribution, mass moment of inertia and large axial forces was taken into account. Numerical experiments have been done concerning the calculation of the eigen-frequencies and eigen-modes of the FGM beams. Murin *et al.* (2012) studied and evaluated the effect of the shear correction function in modal analysis of the FGM beams. Free vibration equations and their solutions was presented including the shear correction function. Furthermore, second order beam effects and longitudinal varying elastic beam foundations were considered. Ziane *et al.* (2012) investigated free vibration of FGM box beam using formulation of an exact dynamic stiffness matrix on the basis of first-order shear deformation theory (FSDT). The proposed model was validated by comparison with finite element analysis for various boundary conditions. This results showed good conformity between the values of Abaqus Analysis and those calculated with the present method. Wei *et al.* (2011) proposed an analytical method for solving free vibration of cracked FGM beams with axial loading using Euler-Bernoulli and Timoshenko theory. The discontinuity of rotation caused by the cracks was simulated by means of the rotational spring. The main advantage of the proposed method was that the eigenvalue equation for vibrating beams with an arbitrary number of cracks can be conveniently determined from a third-order determinant. Also, a comprehensive analysis was conducted to investigate the influences of the location and total number of cracks, material properties, axial load, inertia and end supports on the natural frequencies and vibrational mode shapes of FGM beams. Al-Ansari (2012) calculated the natural frequencies of cantilever stepping beam using Rayleigh model, modified Rayleigh model, and finite elements model (ANSYS model). The comparison between the three methods was presented in this study and the convergence for the three methods was shown. The results showed that natural frequencies of stepping beam increased with increasing the width of small and large parts of beam. In addition, natural frequencies of the beam is increased with increasing the length of large width and decreased when the modified Rayleigh model or ANSYS model was used. Wattanasakulpong and Ungbhakorn (2012) applied differential transformation method (DTM) to investigate free vibration of FGM beams supported by arbitrary boundary conditions. The main advantages of this method are known for its excellence in high accuracy with small computational expensiveness. The new frequencies results and mode shapes of FGM beams resting on elastically end constraints were presented. For elastically end constraints, some available results of special cases for isotropic beams was used to validate the present results. Li *et al.* (2013) derived bending solutions of FGM Timoshenko beams in terms of the homogenous Euler-Bernoulli beams. The deflection, rotational angle, bending moment and shear force of FGM Timoshenko beams was expressed in terms of the deflection of the corresponding homogenous Euler-Bernoulli beams. Consequently, solutions of bending of the FGM Timoshenko beams were simplified as the calculation of the transition coefficients and the geometry of the beams. Aydin (2013) studied free vibration of beams made of FGM containing any arbitrary number of open edge cracks. The study

was based on Euler-Bernoulli beam and massless rotational springs connecting two intact segments of the beam. The frequencies equation for a damaged FGM beam with any kind of two end supports and any arbitrary number of cracks was established through a third order determinant. Compared to previous studies, this decrease in the determinant order can lead to significant advantages in the computational time. Rong and Liang (2014) investigated free vibration of FGM beams with a through-width delamination. The beam was subdivided into three regions and four elements. Then governing equations of the beam segments was derived based on the Timoshenko beam theory and the assumption of constrained mode. By using the differential quadrature element method the natural frequencies of the beam were obtained. They also examined effects of parameters of material gradients, the size and location of delamination on the natural frequencies. Komijani *et al.* (2014) investigated buckling and post-buckling analysis and small amplitude vibrations in the pre/post-buckling regimes of FGM beams resting on a nonlinear elastic foundation and subjected to in-plane thermal loads. Thermo-mechanical properties of the FGM beams were assumed to be functions of both temperature and thickness. The solution was determined in two different regimes. Eventually, influences of nonlinear elastic foundation parameters, thermal load type, different types of boundary conditions, microstructural length scale on equilibrium paths, critical buckling load, and fundamental frequencies were studied. Porous materials with functional properties such as foams have been widely used in industry. Biot (1964), the leader of expression of porous material behavior, studied the fluid-saturated porous plate under the axial force and uniform thermal field. He assumed that pores distributed in all direction uniformly and they had uniform effect on mechanical properties of plate. Buckling of porous beams with varying properties were described by Magnucki and Stasiewicz (2004). They used shear deformation theory for solving the critical load. In this study the effect of porosity on the strength and buckling load of the beam was investigated, too. Magnucki *et al.* (2006) investigated bending and buckling of rectangular plate made of foam material. He obtained the result for a poro/nonlinear symmetric distribution plate. Magnucki *et al.* (2014) investigated on theoretical and experimental study of a sandwich circular plate under pure bending. Buckling of circular porous plate with varying properties and simply supported boundary conditions were described by Magnucka-Blandzi (2008). The researchers obtained the critical buckling load for a poro/nonlinear symmetric distribution plate. He also studied the circular plate without of pore pressure. Dynamic stability of a metal foam circular plate with varying properties were described by Magnucka-Blandzi (2009). Magnucka-Blandzi (2011) obtained the critical buckling load for rectangular plate made of foam with two layers of perfect material. The core was made of a metal foam with properties varying across thickness. Jasion *et al.* (2012) investigated on the analytical, numerical and experimental critical buckling load for plate and beam made of foam with two layers of perfect material. They obtained global and local buckling-wrinkling of the face sheets of sandwich beams and sandwich circular plates. They also compared values of the critical load obtained by analytical, numerical (FEM), and experimental methods. Zimmerman (2000) studied on thermoelastic and poroelastic coupling parameters for a linear poroelastic saturated rock. He concluded that poroelastic coupling parameter has a stronger influence than thermoelastic one. Ghassemi and Zhang (2004) showed the effects of temperature gradients on pore pressure and stress distribution by using an one-isothermal poroelasticity theory. Thereafter Ghassemi (2007) investigated the influence of cooling on pore pressure and stresses distribution by displacement discontinuity method. Jabbari *et al.* (2014a, b) investigated the poroelastic circular plate under the mechanical and thermal forces. They studied the effects of distribution and properties of pores that saturated by fluid on stability of plate. Jabbari *et al.* (2014c, d) considered the stability of sandwich

plate with piezoelectric layers and poroelastic core under uniform thermal and electrical field. Moreover, they achieved their results in higher-order and first-order theory and compared with classic theory. They explored the effects of mechanical and thermal properties on stability of poroelastic plate, too. Mojahedin *et al.* (2014) studied the buckling of poroelastic plate with piezoelectric layers under electrical, thermal and mechanical forces. Jabbari *et al.* (2014e, f) considered the buckling of circular and rectangular poro FGM plate under transverse magnetic field. They explained the effects of mechanical and magnetic properties on stability of poro magnet plate.

In this research free vibration of porous beam is investigated. First, the equations of motions were derived using Euler-Bernoulli theory. Then natural frequencies of porous beam have been obtained in three different boundary conditions: clamped-clamped, clamped-free and hinged-hinged support. Finally, the effects of poroelastic parameters (such as stiffness and mass) and pores compressibility has been considered separately and simultaneously on the natural frequencies.

## 2. Derivation of the governing equations

Consider a beam made of saturated porous materials with rectangular cross section. It is assumed that the length of the beam is  $L$  and cross section is  $b \times h$ . Cartesian coordinates is used such that the  $x$  axis is at the left side of the beam on its middle surface (Fig. 1).

The functional relationship between  $E$  and  $z$  for porous beam is assumed as three different types as:

- (1) Porous material with nonlinear nonsymmetric distribution (PNND): material which has nonlinear asymmetric distribution of porosity in thickness direction and consequently its material properties and Young's modulus are as nonlinear asymmetric form. Here Young's modulus and density are being shown with (Magnucka-Blandzi 2009, Jabbari *et al.* 2014a)

$$E(z) = E_0 \left[ 1 - e_S \cos \left( \left( \frac{\pi}{2h} \right) \left( z + \frac{h}{2} \right) \right) \right] \quad (1a)$$

$$\rho(z) = \rho_0 \left[ 1 - e_M \cos \left( \left( \frac{\pi}{2h} \right) \left( z + \frac{h}{2} \right) \right) \right] \quad (1b)$$

which is a nonlinear asymmetric form of Young's modulus.

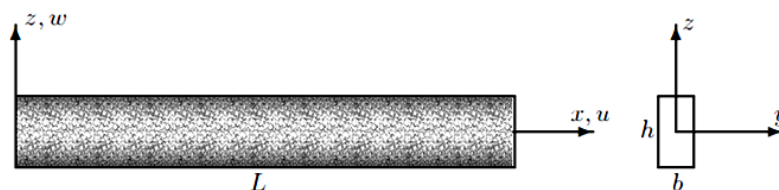


Fig. 1 The geometry and coordinate system of a porous beam

- (2) Porous material with nonlinear symmetric distribution (PNSD): material which has nonlinear symmetric distribution of porosity in thickness direction and consequently its material properties and shear modulus are as nonlinear symmetric form. Here Young’s modulus and density are being shown with

$$E(z) = E_0 \left[ 1 - e_S \cos\left(\frac{\pi z}{h}\right) \right] \tag{2a}$$

$$\rho(z) = \rho_0 \left[ 1 - e_M \cos\left(\frac{z\pi}{h}\right) \right] \tag{2b}$$

- (3) Porous materials with monotonous distribution (PMD): Porous material which has same porosity throughout the porous material and therefore Young’s modulus and density are constant throughout the material as

$$E(z) = E_0 [1 - e_S] \tag{3a}$$

$$\rho(z) = \rho_0 [1 - e_M] \tag{3b}$$

where  $e_S$  and  $e_M$  are the coefficient of beam porosity and mass ( $0 < e_S < 1$  and  $0 < e_M < 1$ ),  $E_1$  and  $E_0$  are Young’s modulus of elasticity at  $z = -h / 2$  and  $z = h / 2$ , respectively. It should be noted that the mechanical properties of the porous material vary across the thickness of the beam and  $E_0$  is Young’s modulus for perfect beam, ( $E_0 \geq E_1$ ).

### 2.1 Stress-strain equation porous beam

The linear poroelasticity theory of Biot has two characteristics (Biot 1964):

- (1) An increase of pore pressure induces a dilation of pore.
- (2) Compression of the pore causes a rise of pore pressure.

The stress-strain law for the undrained condition poroelastic beam is given by (Jabbari *et al.* 2014a)

$$\sigma_{xx} = [E(z) + \alpha^2 \bar{M}(1 - 2\nu_u)] \epsilon_{xx} \tag{4}$$

where

$$\bar{M} = \frac{2G(\nu_u - \nu)}{\alpha^2(1 - 2\nu_u)(1 - 2\nu)} \tag{5}$$

$$\nu_u = \frac{\nu + \alpha B(1 - 2\nu)/3}{1 - \alpha B(1 - 2\nu)/3} \tag{6}$$

where  $\bar{M}$  is Biot’s modulus,  $\nu$  is Poisson’s ratio and is assumed to be constant across thickness of the beam and existence of pores have negligible effect on Poisson’s ratio. So it can be assumed that Poisson’s ratio in discharged state is equal with Poisson’s ratio in homogeneous state.  $\nu_u$  is

undrained Poisson's ratio  $\nu < \nu_u < 0.5$ ,  $\alpha$  is Biot coefficient of effective stress  $0 < \alpha < 1$ , and  $B$  is Skempton coefficient.

The analysis of beam is based on the classical beam theory using Euler-Bernoulli assumptions. The displacement field for Euler-Bernoulli beam is given as

$$\bar{u}(x, z, t) = u(x, t) - zw(x, t)_{,x} \quad (7a)$$

$$\bar{w}(x, t) = w(x, t) \quad (7b)$$

where  $\bar{u}(x, z, t)$  and  $\bar{w}(x, t)$  are displacements of an arbitrary point of the beam along  $x$  and  $z$ -directions, respectively. Also,  $u$  and  $w$  are the displacements of the mid-surface of the beam which are functions of  $x$  and  $t$ . The strain-displacement relations for the beam are given in the form

$$\varepsilon_{xx} = \bar{u}_{,x} \quad (8)$$

where  $\varepsilon_{xx}$  is the axial strain. Substituting Eqs. (7) and (8) into Eq. (4) the axial stress remains along the beam, which is equal to

$$\sigma_{xx} = [E(z) + \alpha^2 \bar{M}(1 - 2\nu_u)](u_{,x} - zw_{,xx}) \quad (9)$$

### 3. Free vibration analysis

By employing the principle of virtual displacement, the equations of motion of porous beam can be obtained as

$$\int_0^t (\delta U - \delta T) dt = 0 \quad (10)$$

where the total virtual strain energy of the beam  $\delta U$  can be written as

$$\delta U = \frac{1}{2} \int_V \sigma_{xx} \delta \varepsilon_{xx} dV \quad (11)$$

Elastic strain energy for porous materials is comprised of elastic strain energy for solid body and fluid in pores. Substituting Eqs. (8) and (9) into Eq. (11) in the undrained condition, strain energy is obtained as

$$\delta U = \frac{1}{2} \int_V [E(z) + \alpha^2 \bar{M}(1 - 2\nu_u)](u_{,x} + zw_{,xx})(\delta u_{,x} + z \delta w_{,xx}) dV \quad (12)$$

The kinetic energy  $\delta T$  is presented as well by

$$\delta T = \frac{1}{2} \int_V \rho(z) \delta u_{,t}^2 dV \quad (13)$$

Substituting Eqs. (12) and (13) into Eq. (10), and using integration by parts in Eq. (10), the following expressions are concluded

$$\delta u : A_1 u_{,xx} - A_2 w_{,xxx} = 0 \tag{14}$$

$$\delta w : A_2 u_{,xxx} - A_3 w_{,xxxx} - I w_{,tt} = 0 \tag{15}$$

Through the integrating process, the natural and essential boundary conditions are achieved as

$$u = \textit{known}, \quad \textit{or} \quad N = A_1 u_{,x} - A_2 w_{,xx} = 0 \tag{16}$$

$$w_{,x} = \textit{known}, \quad \textit{or} \quad M = A_2 u_{,x} - A_3 w_{,xx} = 0 \tag{17}$$

$$w = \textit{known}, \quad \textit{or} \quad Q = A_2 u_{,xx} - A_3 w_{,xxx} = 0 \tag{18}$$

where  $N$  is the stress resultants,  $M$  is the moment resultants and  $Q$  is the shear force resultants normal to the mid-plane, and  $A_1$ ,  $A_2$  and  $A_3$  are stretching, coupling stretching-bending and bending stiffness, respectively. Moreover,  $I$  is the moment of inertia, which can be defined as

$$A(z) = E(z) + \alpha^2 M(1 - 2\nu_u), \quad A_1 = \int_{-h/2}^{h/2} A(z) dz, \quad A_2 = \int_{-h/2}^{h/2} z A(z) dz \tag{19a}$$

$$A_3 = \int_{-h/2}^{h/2} z^2 A(z) dz, \quad I = \int_{-h/2}^{h/2} \rho(z) dz \tag{19b}$$

In this study three possible types of boundary conditions are investigated: clamped-clamped, hinged-hinged and clamped-free. Mathematical expressions for the boundary conditions are:

(1) Clamped-Clamped (C-C)

$$u = 0, \quad w = 0, \quad w_{,x} = 0, \quad \textit{at} \quad x = 0, L \tag{20}$$

(2) Clamped-Free (C-F)

$$u = 0, \quad w = 0, \quad w_{,x} = 0, \quad \textit{at} \quad x = 0 \tag{21a}$$

$$N = 0, \quad M = 0, \quad Q = 0, \quad \textit{at} \quad x = L \tag{21b}$$

(3) Hinged-Hinged (H-H)

$$u = 0, \quad w = 0, \quad M = 0, \quad \textit{at} \quad x = 0, L \tag{22}$$

It should be noted in clamped edge (see Eq. (20))  $u$ ,  $w$  and  $w_x$  are independently zero, so clamped boundary condition is not function of the coefficients of mechanical properties of the beam ( $A_1$ ,  $A_2$ ,  $A_3$ ). Moreover, free edge is function of  $N$ ,  $M$  and  $Q$  (see Eq. (21)). To satisfy free boundary condition,  $u_x$  and  $w_{xx}$  must be zero independently (see Eqs. (16), (17) and (18)). Consequently, this boundary condition is not function of the coefficients of mechanical properties of the beam. On the other hands, according to Eq. (22) in hinged-hinged boundary condition,  $M$  is function of mechanical properties of the beam and,  $u_x$  and  $w_{xx}$  are not zero independently. Hence,

the boundary condition is function of the coefficients of mechanical properties of the beam.

### 3.1 Solution

For harmonic vibrations, the displacements of free vibration of the functionally graded porous Euler-Bernoulli beam can be written as

$$u(x, t) = u(x)e^{i\omega t} \quad (23)$$

$$w(x, t) = w(x)e^{i\omega t} \quad (24)$$

where  $\omega$  is the natural frequency of porous beam. Substituting Eqs. (23) and (24) into Eqs. (14) and (15) leads to the axial displacement and the deflection solution, respectively.

$$u(x) = \lambda \frac{A_2}{A_1} [C_1 \cos(\lambda x) - C_2 \sin(\lambda x) + C_3 \cosh(\lambda x) + C_4 \sinh(\lambda x)] + C_5 x + C_6 \quad (25)$$

$$w(x) = C_1 \sin(\lambda x) - C_2 \cos(\lambda x) + C_3 \sinh(\lambda x) + C_4 \cosh(\lambda x) \quad (26)$$

where

$$\lambda^4 = \frac{\omega^2 I}{A_3 - \frac{A_2^2}{A_1}} \quad (27)$$

$C_1, C_2, C_3, C_4, C_5$  and  $C_6$  are constants which depend on boundary conditions on both sides of the beam. The characteristic equation obtains by substituting Eqs. (25) and (26) into Eqs. (20), (21) and (22) as follow

$$[H(\omega)]\{F\} = \{0\} \quad (28)$$

where  $[H(\omega)]$  and  $\{F\}$  are coefficient matrix and unknown matrix, respectively (see Appendix A). Considering Eq. (28), a non-trivial solution is obtained by setting the determinant of the coefficient matrix equal to zero, which results in finding the bending natural frequencies of the beam.

## 4. Results and discussion

In this study the free vibration of porous beam with functional texture has been studied using Euler-Bernoulli theory in various boundary conditions. Because of small deformation of beam, characteristics of pores are independent of beam deformation. Also, the characteristics are constant during beam deformation and do not vary by changing original characteristics of beam. Moreover, the effect of poroelastic material properties on natural frequencies of the beam has been investigated.  $(\bar{\omega})$  is considered relative natural frequency of the beam which is dimensionless parameter as follow

$$\bar{\omega} = \frac{\omega}{\omega_H} = \sqrt{\frac{I_H}{I} \left( \frac{A_3}{A_{3H}} \right) [1 - (A_2/A_3)(A_2/A_1)]} \quad (29)$$

Where  $\omega$  and  $\omega_H$  are natural frequency of porous beam and natural frequency of homogeneous beam with the same boundary condition, respectively. Generally, homogeneous beam is a beam which is formed of a material with the same mechanical properties in all directions.

One of the poroelastic properties of porous beam is existence of pores. Increasing the porosity causes decrement of the Young's modulus and stiffness of beam. On the other hands, natural frequencies are proportional to the stiffness and conversely proportional with mass of beam. Figs. 2-4 show the effect of porosity coefficient on natural frequencies of the beam in hinged-hinged, clamped-clamped and free-clamped boundary conditions. As be seen in these figures, by growing the porosity, stiffness and natural frequencies have declined. In Fig. 2 the first, second and third frequencies of poroelastic beam with hinged-hinged boundary condition are shown. According to

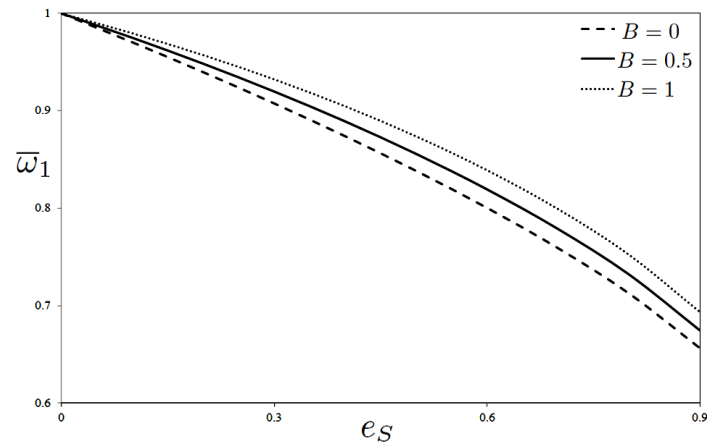


Fig. 2(a) First normalized natural frequency ( $\bar{\omega}_1$ ) vs. coefficient of beam porosity ( $e_s$ ) for saturated porous beam with H-H edges and for the cases of Skempton [ $B = 0, 0.5, 1$ ], coefficient of beam mass  $e_M = 0$  and  $\nu = 0.3$

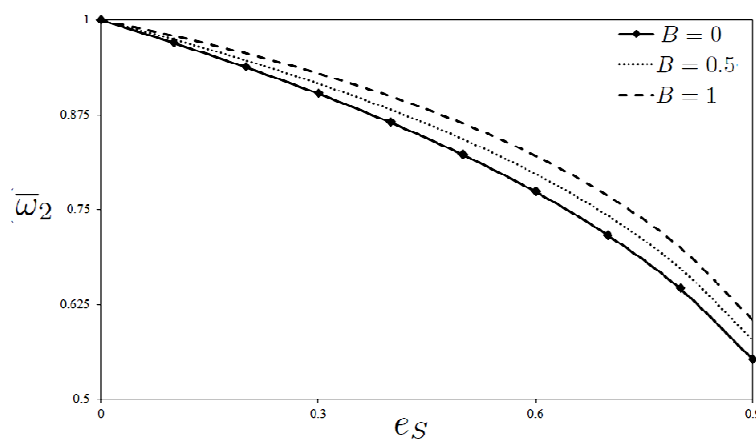


Fig. 2(b) Second normalized natural frequency ( $\bar{\omega}_2$ ) vs. coefficient of beam porosity ( $e_s$ ) for saturated porous beam with H-H edges and for the cases of Skempton [ $B = 0, 0.5, 1$ ], coefficient of beam mass  $e_M = 0$  and  $\nu = 0.3$

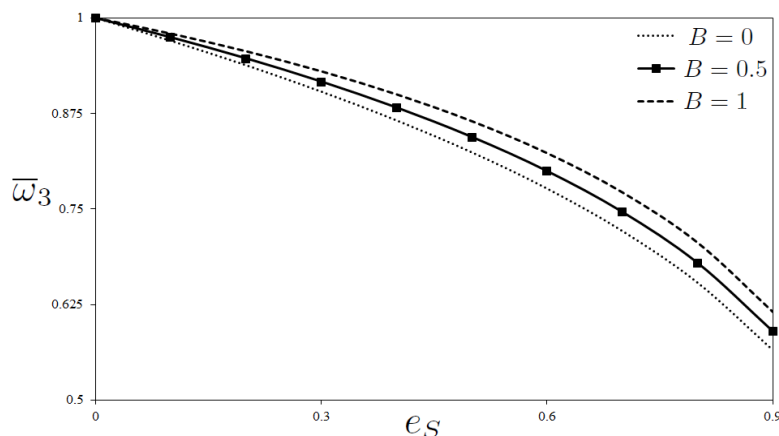


Fig. 2(c) Third normalized natural frequency ( $\bar{\omega}_3$ ) vs. coefficient of beam porosity ( $e_S$ ) for saturated porous beam with H-H edges and for the cases of Skempton [ $B = 0, 0.5, 1$ ], coefficient of beam mass  $e_M = 0$  and  $\nu = 0.3$

Eq. (22), the boundary condition depends on  $A_2$  and  $A_3$  and these coefficients depend on properties of the beam. As a result, the proportion of natural frequencies of porous beam to the natural frequency of homogeneous beam does not change equally. So, the graphs of these frequencies ( $w_1, w_2, w_3$ ) do not coincide to each other. On the other hand, C-C and C-F boundary conditions are not dependent on  $A_2$  and  $A_3$ . So, in this case, ( $\bar{\omega}$ ) is equal for all mode shapes and considering only one of natural frequency ratio is enough for drawing the relevant diagrams (see Figs. 3-6).

Figs. 3 and 4 show the poroelastic beam frequencies with clamped-clamped and clamped-free boundary condition. As can be observed in these figures, by increasing coefficient of beam porosity, the natural frequencies will be decreased. Also, the effect of pores compressibility on natural frequencies of poroelastic beam is presented in Figs. 2-4.

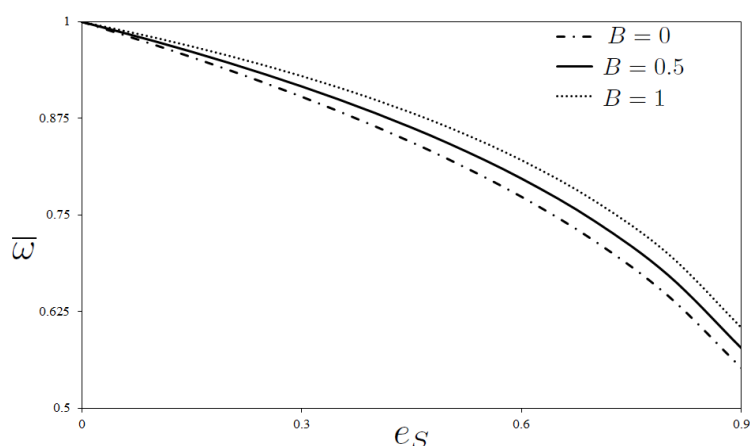


Fig. 3 Normalized natural frequency ( $\bar{\omega}$ ) vs. coefficient of beam porosity ( $e_S$ ) for saturated porous beam with C-C edges and for the cases of Skempton [ $B = 0, 0.5, 1$ ], coefficient of beam mass  $e_M = 0$  and  $\nu = 0.3$

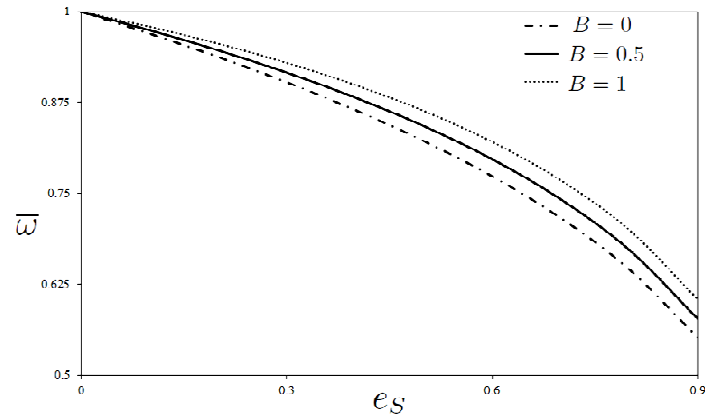


Fig. 4 Normalized natural frequency ( $\bar{\omega}$ ) vs. coefficient of beam porosity ( $e_s$ ) for saturated porous beam with C-F edges and for the cases of Skempton [ $B = 0, 0.5, 1$ ], coefficient of beam mass  $e_M = 0$  and  $\nu = 0.3$

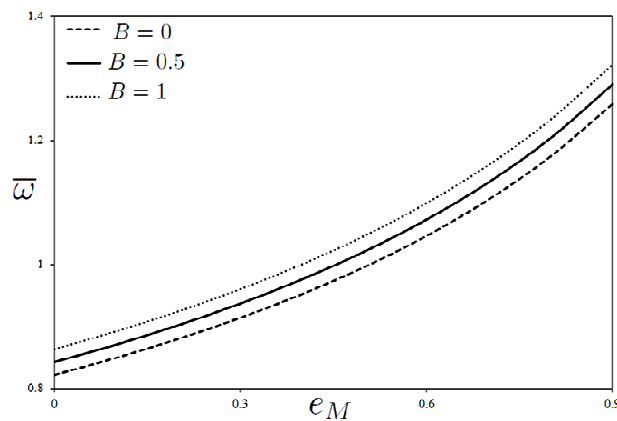


Fig. 5 Normalized natural frequency ( $\bar{\omega}$ ) vs. coefficient of beam mass ( $e_M$ ) for saturated porous beam with C-C edges and for the cases of Skempton [ $B = 0, 0.5, 1$ ], coefficient of beam porosity  $e_s = 0.5$  and  $\nu = 0.3$

In porous materials the compressibility of pores is introduced by Skempton coefficient. If the compressibility of pores is increased Skempton coefficient will be decreased ( $B \rightarrow 0$ ), and the natural frequencies of the beam will be decreased, too. On the contrary, if the compressibility of pores is decreased the Skempton coefficient will be increased ( $B \rightarrow 1$ ), and the natural frequencies of the beam will be increased.

The amount of saturation of pores is expressed by ( $e_M$ ). It should be noted that  $e_M$  differs from Skempton coefficient. To express the difference between these coefficient, it is noteworthy that  $e_M$  only considers the pores density, but Skempton coefficient states the pores compressibility. On the other hand, the pores maybe saturated by fluids with different density or size of pores are not equal. Fig. 5 shows the effect of mass coefficient on natural frequencies. As can be seen in this figure if the coefficient of mass increases, density of beam will decrease, and natural frequencies will increase, because density is proportional conversely with natural frequencies. Mass and porosity

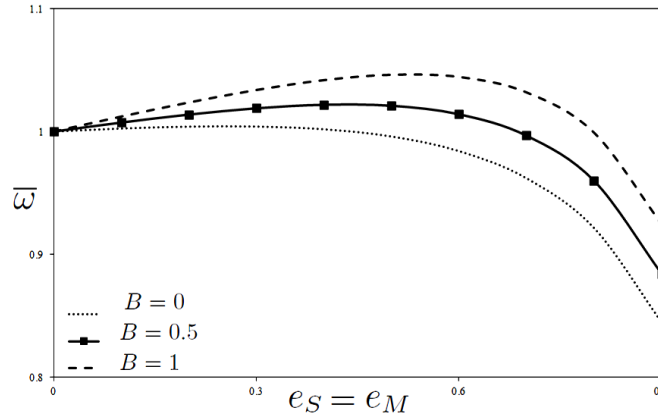


Fig. 6 Normalized natural frequency ( $\bar{\omega}$ ) vs. coefficient of beam mass and porosity ( $e_M, e_S$ ) for saturated porous beam with C-C edges and for the cases of Skempton [ $B = 0, 0.5, 1$ ]

coefficients are independent together, but in some cases both of them change with a same ratio. In Figs. 6 and 7 the effect of both of them on the natural frequencies is shown simultaneously. The figures show that by increasing of these coefficients, natural frequencies of poroelastic beam increase gradually at first. Then, natural frequencies decrease with sharp slope. Since the influence of coefficient of mass is greater than coefficient of porosity, increasing of coefficient of mass rises the natural frequencies. Moreover, by increasing the compressibility ( $B \rightarrow 0$ ), stiffness declines and the graphs are growing by slower slope. In high porosity the effect of stiffness is larger than the effect of coefficient of mass and it causes that natural frequencies decline with sharp slope.

The influence of coefficient of mass is shown in Fig. 7(a) conspicuously. As can be seen, at first, natural frequencies of the porous are increasing gradually until high porosities. Also, the figure shows that first natural frequencies of hinged-hinged edge are different from other natural frequencies and boundary conditions that relationship of natural frequency of hinged-hinged beam to mechanical properties of porous material causes this behavior (see Eq. (22)).

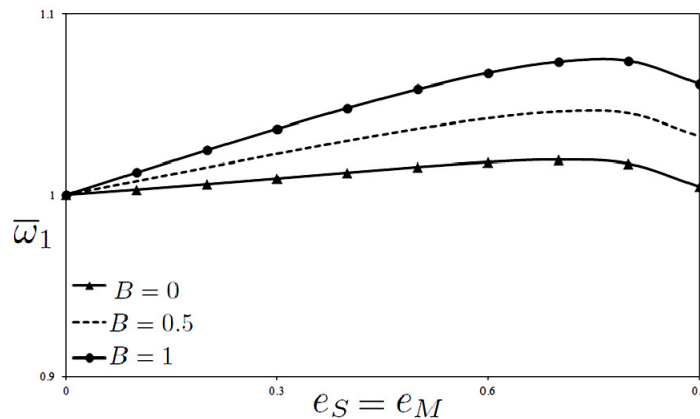


Fig. 7(a) First normalized natural frequency ( $\bar{\omega}_1$ ) vs. coefficients of beam mass and porosity ( $e_M, e_S$ ) for saturated porous beam with H-H edges and for the cases of Skempton [ $B = 0, 0.5, 1$ ]

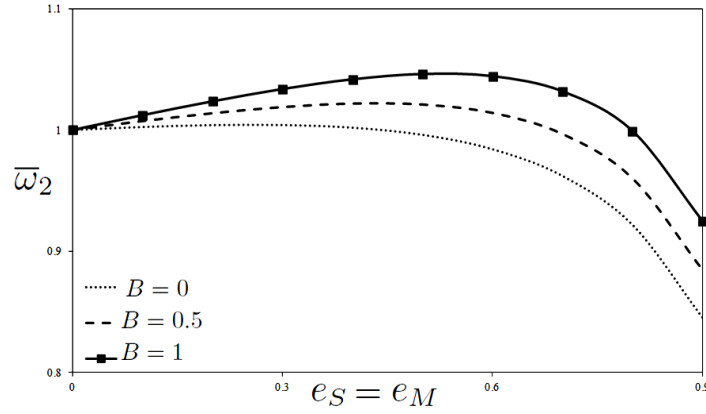


Fig. 7(b) Second normalized natural frequency ( $\bar{\omega}_2$ ) vs. coefficients of beam mass and porosity ( $e_M, e_S$ ) for saturated porous beam with H-H edges and for the cases of Skempton [ $B = 0, 0.5, 1$ ]

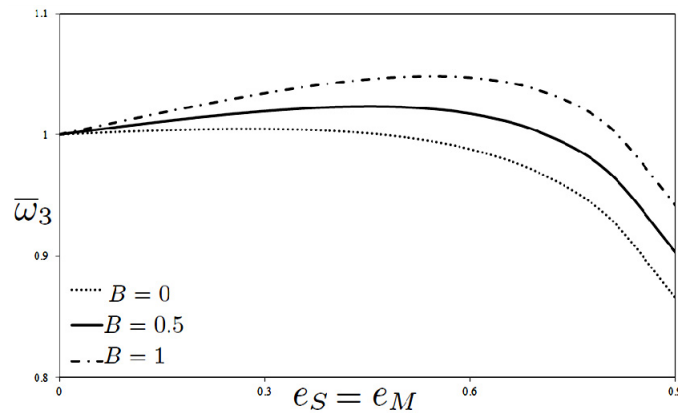


Fig. 7(c) Third normalized natural frequency ( $\bar{\omega}_3$ ) vs. coefficients of beam mass and porosity ( $e_M, e_S$ ) for saturated porous beam with H-H edges and for the cases of Skempton [ $B = 0, 0.5, 1$ ]

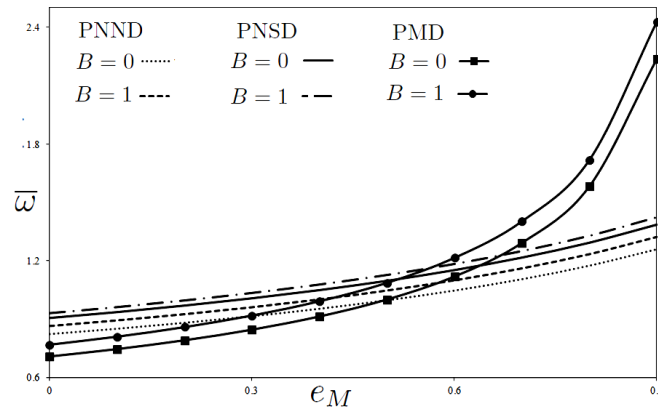


Fig. 8 Normalized natural frequency ( $\bar{\omega}$ ) vs. coefficient of beam mass ( $e_M$ ) for saturated porous beam with C-C edges and for the cases of poro/nonlinear nonsymmetric distribution (PNND), poro/nonlinear symmetric distribution (PNSD) and poro/monotonous distribution (PMD) with  $e_S = 0.5$ , and  $B = 0, 1$

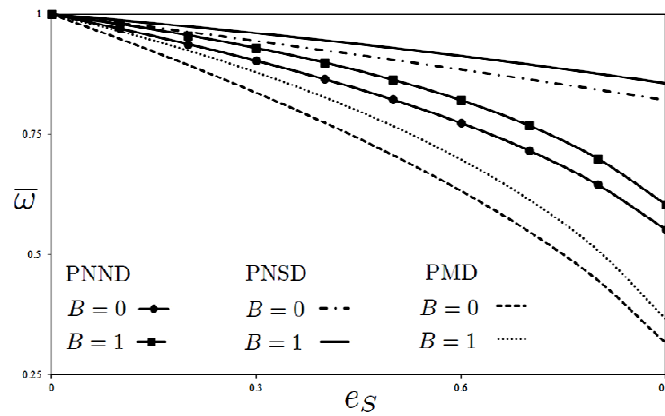


Fig. 9 Normalized natural frequency ( $\bar{\omega}$ ) vs. coefficient of beam porosity ( $e_S$ ) for saturated porous beam with C-C edges and for the cases of poro/nonlinear nonsymmetric distribution (PNND), poro/nonlinear symmetric distribution (PNSD) and poro/monotonous distribution ((PMD) whit  $e_M = 0$ , and  $B = 0, 1$

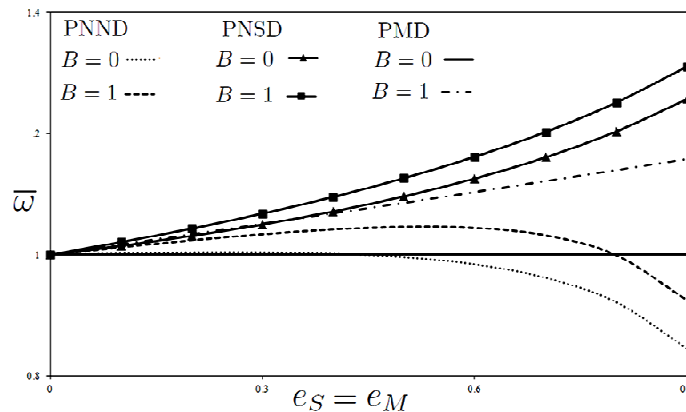


Fig. 10 Normalized natural frequency ( $\bar{\omega}$ ) vs. coefficients of beam mass and porosity ( $e_M, e_S$ ) for saturated porous beam with C-C edges and for the cases of poro/nonlinear nonsymmetric distribution (PNND), poro/nonlinear symmetric distribution (PNSD) and poro/monotonous distribution ((PMD) whit  $B = 0, 1$

Figs. 8-10 show the poro nonlinear distribution in symmetric, nonsymmetric and monotonous. At first sight, it can be clearly seen that porous distribution has large effect on natural frequencies of the beam. According to Fig. 8 mass coefficient has the most influence on natural frequencies in monotonous distribution which has two reasons: (1) decoupled equations and shear forces have no effect on natural frequencies of beam. (2) In this case, stiffness of beam is lower than the other cases (with the same porosity). Fig. 9 shows saturated porous beam in different porosity distributions ( $e_M = 0$ ). As the graph shows the monotonous distribution has the lowest frequency and the most variations due to porosity. On the other hand, in symmetric case, natural frequencies are larger than two other cases because the stiffness is lager in this case. As can be seen in Fig. 10, the results of monotonous and symmetric cases are different from nonsymmetric case, inasmuch as

shear forces in uniform and symmetric cases are zero. Furthermore, the coefficient of mass in these cases is more effective than porosity and the graphs are increasing thoroughly. In monotonous distribution for ( $B = 0$ ), Poisson's ratio is constant and since the effect of porosity on Poisson's ratio of beam is assumed negligible, the graph is consistent to homogenous graph. Therefore, in this case the natural frequencies of porous beam and homogeneous beam are the same.

## 5. Conclusions

In the present study, the free vibration analysis of beam made of porous material was investigated. First, the energy method based on the Euler-Bernoulli beam is used for deriving the governing equation of motion. In Euler-Bernoulli theory transverse shear stress and strain is being neglected which simplify the problem for thin beams and the results in admissible answer. In free vibration analysis the effect of transverse shear stress is considerable but it has been shown that the results of Euler-Bernoulli theory are close to Timoshenko theory and higher order shear deformation theory for thin beams which can be used as a useful method for analyzing vibrational problems. The boundary conditions of the beam were assumed to be clamped-clamped, clamped-free and hinged-hinged. The porous beam which pores are saturated with fluid. Then, the effect of pores distribution and compressibility of pores on the natural frequencies are investigated. The effects of porosity on natural frequencies of rectangular beam as closed-form solution are presented. It is concluded that:

- Natural frequency ratio ( $\bar{\omega}$ ) has equal value for each beam with special mechanical properties, unless the right hand of the Eq. (29) (coefficients  $A_1, A_2, A_3$ ) would be function of mode shapes of the beam.
- By increasing the coefficient of porosity  $e_S$  the natural frequency ( $\omega$ ) will be reduced.
- By increasing the coefficient of mass  $e_M$  the natural frequency ( $\omega$ ) will be increased.
- By increasing the compressibility of fluid within the pores, the natural frequency ( $\omega$ ) will be reduced.
- In porous materials method of the pores distribution is impressive on the strength of porous beam and natural frequencies ( $\omega$ ). In each case of pores distribution and boundary conditions, different results have been achieved.
- The moment resultants ( $M$ ) is a function of the Skempton coefficient ( $B$ ) and porosity coefficients ( $e_S$ ). Accordingly, natural frequencies ( $\omega$ ) of hinged-hinged beam is a function of them.
- The behavior of natural frequencies of hinged-hinged beam are different from beam with two other boundary conditions.

## References

- Al-Ansari, L.S. (2012), "Calculating of natural frequency of stepping cantilever beam", *International J. Mech. Mechatron. Eng.*, **12**(5), 59-68.
- Aminbaghai, M., Murin, J. and Kuti, V. (2012), "Modal analysis of the FGM-beams with continuous transversal symmetric and longitudinal variation of material properties with effect of large axial force", *Eng. Struct.*, **34**, 314-329.
- Aydin, K. (2013), "Free vibration of functionally graded beams with arbitrary number of surface cracks",

- Euro. J. Mech. A/Solids*, **42**, 112-124.
- Biot, M.A. (1964), "Theory of buckling of a porous slab and its thermoelastic analogy", *J. Appl. Mech.*, **31**(2), 194-198.
- Ghassemi, A. (2007), "Stress and pore pressure distribution around a pressurized, cooled crack in low permeability rock", *Proceedings of the 32nd Workshop on Geothermal Reservoir Engineering Stanford University*, Stanford, CA, USA, January-February.
- Ghassemi, A. and Zhang, Q. (2004), "A transient fictitious stress boundary element method for porothermoelastic media", *Eng. Anal. Boundary Elem.*, **28**(11), 1363-1373.
- Jabbari, M., Mojahedin, A., Khorshidvand, A.R. and Eslami, M.R. (2014a), "Buckling analysis of a functionally graded thin circular plate made of saturated porous materials", *J. Eng. Mech.*, **140**(2), 287-295.
- Jabbari, M., Hashemitaheri, M., Mojahedin, A. and Eslami, M.R. (2014b), "Thermal buckling analysis of functionally graded thin circular plate made of saturated porous materials", *J. Therm. Stresses*, **37**(2), 202-220.
- Jabbari, M., Farzaneh Joubaneh, E. and Mojahedin, A. (2014c), "Thermal buckling analysis of porous circular plate with piezoelectric actuators based on first order shear deformation theory", *Int. J. Mech. Sci.*, **83**, 57-64.
- Jabbari, M., Mojahedin, A. and Farzaneh Joubaneh, E. (2014d), "Thermal buckling analysis of circular plates made of piezoelectric and saturated porous functionally graded material layers", *J. Eng. Mech.*, **141**(4), 287-295.
- Jabbari, M., Mojahedin, A. and Haghi, M. (2014e), "Buckling analysis of thin circular FG plates made of saturated porous-softferro magnetic materials in transverse magnetic field", *Thin-Wall. Struct.*, **85**, 50-56.
- Jabbari, M., Haghi, M. and Mojahedin, A. (2014f), "Buckling analysis of thin rectangular FG plates made of saturated porous-softferro magnetic materials in transverse magnetic field", *J. Solid Mechanics*, **85**, 50-56.
- Jasion, P., Magnucka-Blandzi, E., Szyk, W. and Magnucki, K. (2012), "Global and local buckling of sandwich circular and beam-rectangular plates with metal foam core", *Thin-Wall. Struct.*, **61**, 154-161.
- Komijani, M., Esfahani, S.E., Reddy, J.N., Liu, Y.P. and Eslami, M.R. (2014), "Nonlinear thermal stability and vibration of pre/post-buckled temperature and microstructure dependent FGM beams resting on elastic foundation", *Compos. Struct.*, **112**, 297-307.
- Li, S.R., Cao, D.F. and Wan, Z.Q. (2013), "Bending solutions of FGM Timoshenko beams from those of the homogenous Euler-Bernoulli beams", *Appl. Math. Model.*, **37**(10-11), 7077-7085.
- Magnucka-Blandzi, E. (2008), "Axi-symmetrical deflection and buckling of circular porous-cellular plate", *Thin-Wall. Struct.*, **46**(3), 333-337.
- Magnucka-Blandzi, E. (2009), "Dynamic stability of a metal foam circular plate", *J. Theor. Appl. Mech.*, **47**(2), 421-433.
- Magnucka-Blandzi, E. (2011), "Mathematical modeling of a rectangular sandwich plate with metal foam core", *J. Theor. Appl. Mech.*, **49**(2), 439-455.
- Magnucki, K. and Stasiewicz, P. (2004), "Elastic buckling of a porous beam", *J. Theor. Appl. Mech.*, **42**(4), 859-868.
- Magnucki, K., Malinowski, M. and Kasprzak, J. (2006), "Bending and buckling of a rectangular porous plate", *Steel Compos. Struct., Int. J.*, **6**(4), 319-333.
- Magnucki, K., Jasion, P., Magnucka-Blandzi, E. and Wasilewicz, P. (2014), "Theoretical and experimental study of a sandwich circular plate under pure bending", *Thin-Wall. Struct.*, **79**, 1-7.
- Mojahedin, A., Farzaneh Joubaneh, E. and Jabbari, M. (2014), "Thermal and mechanical stability of a circular porous plate with piezoelectric actuators", *Acta Mechanica*, **225**(12), 3437-3452.
- Murin, J., Aminbaghai, M. and Kuti, V. (2010), "Exact solution of the bending vibration problem of FGM beams with variation of material properties", *Eng. Struct.*, **32**, 1631-1640.
- Murin, J., Aminbaghai, M., Hrabovsky, J., Kuti, V. and Kugler, S. (2012), "Modal analysis of the FGM beams with effect of the shear correction function", *Compos.: Part B*, **45**, 1575-1582.
- Rong, L.S. and Liang, F.L. (2014), "Free vibration of FGM Timoshenko beams with through-width delamination", *Sci. China Phys. Mech. Astron.*, **57**(5), 927-934.

- Wattanasakulpong, N. and Ungbhakorn, V. (2012), "Free vibration analysis of functionally graded beams with general elastically end constraints by DTM", *World J. Mech.*, **2**(6), 297-310.
- Wei, D., Liu, Y. and Xiang, Z. (2011), "An analytical method for free vibration analysis of functionally graded beams with edge cracks", *J. Sound Vib.*, **331**(7), 1686-1700.
- Ziane, N., Meftah, S.A., Belhadj, H.A., Tounsi, A. and Bedia, A.A. (2012), "Free vibration analysis of thin and thick-walled FGM box beams", *Int. J. Mech. Sci.*, **66**, 273-282.
- Zimmerman, R.W. (2000), "Coupling in poroelasticity and thermoelasticity", *Int. J. Rock Mech. Mining. Sci.*, **37**(1-2), 79-87.

CC

## Appendix A

$[H(\omega)]$  can be written as follows:

$$H(\omega) = \begin{bmatrix} \lambda \frac{A_2}{A_1} & 0 & \lambda \frac{A_2}{A_1} & 0 & 0 & 1 \\ 0 & 1 & 0 & 1 & 0 & 0 \\ \lambda & 0 & \lambda & 0 & 0 & 0 \\ 0 & 0 & 0 & 0 & A_1 & 0 \\ \lambda^2 g \sin(\lambda L) & \lambda^2 g \cos(\lambda L) & -\lambda^2 g \sinh(\lambda L) & -\lambda^2 g \cosh(\lambda L) & A_2 & 0 \\ \lambda^3 g \cos(\lambda L) & -\lambda^3 g \sin(\lambda L) & -\lambda^3 g \cosh(\lambda L) & -\lambda^3 g \sinh(\lambda L) & 0 & 0 \end{bmatrix}$$

for the functionally graded porous beams by clamped-clamped boundary condition, and

$$H(\omega) = \begin{bmatrix} \lambda \frac{A_2}{A_1} & 0 & \lambda \frac{A_2}{A_1} & 0 & 0 & 1 \\ 0 & 1 & 0 & 1 & 0 & 0 \\ \lambda & 0 & \lambda & 0 & 0 & 0 \\ 0 & 0 & 0 & 0 & A_1 & 0 \\ \lambda^2 g \sin(\lambda L) & \lambda^2 g \cos(\lambda L) & -\lambda^2 g \sinh(\lambda L) & -\lambda^2 g \cosh(\lambda L) & A_2 & 0 \\ \lambda^3 g \cos(\lambda L) & -\lambda^3 g \sin(\lambda L) & -\lambda^3 g \cosh(\lambda L) & -\lambda^3 g \sinh(\lambda L) & 0 & 0 \end{bmatrix}$$

for the functionally graded porous beams by clamped-free boundary condition, and

$$H(\omega) = \begin{bmatrix} \lambda \frac{A_2}{A_1} & 0 & \lambda \frac{A_2}{A_1} & 0 & 0 & 1 \\ 0 & 1 & 0 & 1 & 0 & 0 \\ 0 & \lambda^2 g & 0 & -\lambda^2 g & A_2 & 0 \\ \lambda \frac{A_2}{A_1} \cos(\lambda L) & -\lambda \frac{A_2}{A_1} \sin(\lambda L) & \lambda \frac{A_2}{A_1} \cosh(\lambda L) & \lambda \frac{A_2}{A_1} \sinh(\lambda L) & L & 1 \\ \sin(\lambda L) & \cos(\lambda L) & \sinh(\lambda L) & \cosh(\lambda L) & 0 & 0 \\ \lambda^2 g \sin(\lambda L) & \lambda^2 g \cos(\lambda L) & -\lambda^2 g \sinh(\lambda L) & -\lambda^2 g \cosh(\lambda L) & A_2 & 0 \end{bmatrix}$$

for the functionally graded porous beams by hinged-hinged boundary condition, where

$$g = A_3 - \frac{(A_2)^2}{A_1}$$